

# Applying an Appropriate Cap in an Elastoplastic Model with Open Bounding and Yield Surfaces at High Pressures

Heidarzadeh Heisam<sup>1</sup>, Oliaei Mohammad<sup>1\*</sup> and Latifi Manoocher<sup>2</sup>

<sup>1</sup>Department of Civil & Environmental Engineering, Tarbiat Modares University, Tehran, Iran; H.Heidarzadeh@modares.ac.ir, M.Olyaei@modares.ac.ir

<sup>2</sup>Faculty of Civil Engineering, University of Tehran, Tehran, Iran; mlatifi@ut.ac.ir

## Abstract

**Background:** In some projects such as dam construction, soil experiences changes to some an extent as a result of high pressures. The majority of constitutive models used in geotechnical engineering research specifically for sand are presented without cap which they fail to show the actual plastic behavior of soils at high levels of stresses. In our research, a powerful elastoplastic model from the family of bounding surface plasticity which has an open conical yield surface as well as bounding surface is selected. This model is able to show the plastic behavior of sand in deviatoric loadings very well. However, when confining stress increases, it cannot simulate the plastic behavior of sand specimens especially at high pressures. Here, by introducing an appropriate algorithm for cap, model formulation is developed and modified. It is accomplished by introducing a secondary plasticity mechanism and a yield surface for cap which closes deviatoric yield and bounding surfaces along with the hydrostatic axis. Finally, validity of the model predictions is evaluated with some experimental data available in literature and capabilities of the modified constitutive model with cap are shown at high levels of the stress. These experimental data are provided for Toyoura and Nevada sand; and it is observed that prediction of the constitutive model modified with cap is significantly more satisfactory at high pressures.

**Keywords:** Cap, Constitutive Model, Fabric Changes, High Pressures, Plasticity, Sand

## 1. Introduction

At the present, by advances in computer and technology, numerical analysis and simulation of complex problems of soil mechanics has been made possible<sup>1,2</sup>. Therefore, validity of the prediction of soil behavior in geotechnical problems is mainly dependent on the accuracy and realistic results of the constitutive models and there is no lack of power to compute the models algorithm. The constitutive models presented by Manzari<sup>3</sup> and Manzari and Dafalias<sup>4</sup> are two elastoplastic models which are presented in the framework of bounding surface plasticity. Yield and bounding surfaces of these models are in the form of a cone with open end. Hence, these models are able to show the plastic behavior of sand in shear deformations. However, because of the open end of the yield

surface in these models (ignoring the cap), conditions of fracture (crush) in specimens as a result of increase in the confining stress is not observed. In other words, when the confining stress increases individually and stress path moves along with hydrostatic line, these models can never show the yield behavior of the soil samples and the behavior is assumed to be completely elastic. However, since at very high levels of hydrostatic stresses such as those occurring in lower layers of the large dams, considerable plastic behavior is observed in soils which cannot be simulated by means of models without a cap or with an ordinary cap. As you know, the problems related to dams are considered by many researches such as<sup>5</sup>.

In the metal or plastic materials whose porosity (void ratio) is low, it is assumed that the behavior of the materials is solely elastic during hydrostatic loading. However,

\*Author for correspondence

in aggregate materials such as soil, whose porosity is of higher importance, according to experimental data, it is observed that as confining loading increases, considerable plastic deformations will be occurred specifically in sandy soils at high pressures. This plastic behavior is attributed mainly to failure (crush) in coarser particles, slide of particles on each other and change in the fabric of the aggregate specimens in high levels of stresses (Lacy and Prevost<sup>6</sup>). Consequently, in this paper, it is attempted to overcome this problem by adding a cap so that these constitutive models can present the actual behavior of sand in hydrostatic loading. For this purpose, a secondary plasticity mechanism is defined as the cap yield surface along with the primary mechanism (yield and deviatoric surfaces) so that cap closes the primary yield surface (cone) on the hydrostatic axis.

Herein, each of the plasticity mechanisms (that is, the first mechanism which is in fact a deviatoric mechanism presented by Manzari<sup>3</sup> and Manzari and Dafalias<sup>4</sup> and the second one corresponds to the cap presented in this paper) individually have yield, flow and hardening criteria. Under various loading conditions, aforesaid mechanisms may act together or separately. In this paper, structure of the cap is described and evaluated using various experimental data. These experimental data are provided by<sup>7</sup> for Toyoura and by Salazar<sup>8</sup> for Nevada sand and are available in literature. Finally, it is observed that prediction of the modified constitutive model with cap is significantly more satisfactory than it's done by the main constitutive model (without cap) at high pressures. Also, the predicted data by modified model is relatively fitted to the observed in experimental tests.

## 2. Constitutive Model

As you know, the general form of an elastoplastic constitutive model is as follows:

$$d\sigma'_{ij} = E_{ijkl} \cdot (d\varepsilon_{ij} - d\varepsilon_{ij}^p) \quad (1)$$

where,  $d\sigma'_{ij}$  is the tensor of incremental effective stress,  $d\varepsilon_{ij}$  is the tensor of incremental overall strain,  $d\varepsilon_{ij}^p$  is the tensor of plastic strain and  $E_{ijkl}$  is the tensor of elastic coefficient.

$$E_{ijkl} = (k - \frac{2G}{3})\delta_{ij}\delta_{kl} + G(\delta_{ik}\delta_{jl} + \delta_{il}\delta_{jk}) \quad (2)$$

where,  $K$  is the bulk modulus,  $G$  is the shear modulus and  $\delta_{ij}$  is the Kronecker delta.

Here, the incremental plastic strain components is divided into two parts:

$$d\varepsilon_{ij}^p = d\varepsilon_{ij}^{p1} + d\varepsilon_{ij}^{p2} \quad (3)$$

$d\varepsilon_{ij}^{p1}$  is the incremental plastic strain tensor which is obtained from the first mechanism,  $d\varepsilon_{ij}^{p2}$  is the incremental plastic strain tensor corresponding to the second mechanism resulted from the hydrostatic pressure (volumetric loading). It is assumed that the rate of plastic deformations due to the first and second mechanisms are determined using the following relationships.

$$d\varepsilon_{ij}^{p1} = \langle \lambda_1 \rangle R_{ij} \text{ and } d\varepsilon_{ij}^{p2} = \langle \lambda_2 \rangle R_{ij} \quad (4)$$

where,  $R_{ij}$  is a symmetric second order tensor which denotes the direction of plastic deformations in stress spaces. Moreover,  $\lambda_1$  and  $\lambda_2$  are called plastic loading indices and  $\langle x \rangle$  is known as the McCauley bracket.

$$\langle x \rangle = \begin{cases} x & , \text{ if } x > 0 \\ 0 & , \text{ if } x \leq 0 \end{cases} \quad (5)$$

Both plastic loading indices are defined as follows:

$$\lambda_2 = \frac{1}{H_2^p} L_{ij}^2 \cdot d\sigma_{ij} \text{ and } \lambda_1 = \frac{1}{H_1^p} L_{ij}^1 \cdot d\sigma_{ij} \quad (6)$$

$L_{ij}^1$  and  $L_{ij}^2$  are two tensors defining vectors normal to the conical yield surface and cap yield surface, respectively,  $H_1^p$  and  $H_2^p$  are the plastic moduli corresponding to the mechanism of deviatoric and volumetric yield surfaces, respectively.

$$\lambda_1 = \frac{(H_2^p + H_2^0) \cdot (L_{ij}^1 \cdot E_{ijkl} \cdot d\varepsilon_{kl}) - (L_{ij}^1 \cdot E_{ijkl} \cdot R_{kl}) \cdot (L_{ij}^2 \cdot E_{ijkl} \cdot d\varepsilon_{kl})}{(H_1^p + H_1^0)(H_2^p + H_2^0) - (L_{ij}^1 \cdot E_{ijkl} \cdot R_{kl}) \cdot (L_{ij}^2 \cdot E_{ijkl} \cdot R_{kl})} \quad (7a)$$

$$\lambda_2 = \frac{(H_1^p + H_1^0) \cdot (L_{ij}^2 \cdot E_{ijkl} \cdot d\varepsilon_{kl}) - (L_{ij}^2 \cdot E_{ijkl} \cdot R_{kl}) \cdot (L_{ij}^1 \cdot E_{ijkl} \cdot d\varepsilon_{kl})}{(H_1^p + H_1^0)(H_2^p + H_2^0) - (L_{ij}^1 \cdot E_{ijkl} \cdot R_{kl}) \cdot (L_{ij}^2 \cdot E_{ijkl} \cdot R_{kl})} \quad (7b)$$

where,  $H_2^0 = L_{ij}^2 \cdot E_{ijkl} \cdot R_{kl}$  and  $H_1^0 = L_{ij}^1 \cdot E_{ijkl} \cdot R_{kl}$ .

Eq. 7 a and b apply when the current position of the stress is located over the interface of the cap and deviatoric yield surfaces; i.e., when two mechanisms work simultaneously. According to Manzari<sup>3</sup>, Manzari and Dafalias<sup>4</sup>, Heidarzadeh<sup>9</sup> and Heidarzadeh and Latifi<sup>10</sup>, if  $\lambda_2 = 0$ ,  $\lambda_1$  is defined as follows:

$$\lambda_1 = \frac{L_{ij}^1 \cdot E_{ijkl} \cdot d\varepsilon_{kl}}{H_1^p + H_1^0} \quad (8)$$

Furthermore, for the case in which only the cap yield surface (volumetric surface) acts; i.e. under high level

of hydrostatic pressures without deviatoric loading, the plastic loading indices will be obtained as follows:

$$\lambda_2 = \frac{I_{ij}^2 \cdot E_{ijkl} \cdot d\epsilon_{kl}}{(H_2^p + H_2^0)} \text{ and } \lambda_1 = 0 \tag{9}$$

Substituting Eq. 3, 4 and 7 in Eq. 1, it can be written as:

$$d\sigma_{ij} = E_{ijkl} \cdot d\epsilon_{kl} - (< \lambda_1 > + < \lambda_2 >) \cdot E_{ijkl} \cdot R_{kl} \tag{10}$$

### 2.1 Plastic Modulus

Plastic modulus corresponding to deviatoric loading is defined well by Manzari<sup>3</sup> and Manzari and Dafalias<sup>4</sup> according to the distance of the stress from the deviatoric bounding surface. However, in this research, to define a relationship for plastic modulus in hydrostatic loading corresponding to cap, soil behavior must be first investigated theoretically in a completely hydrostatic loading.

As stated earlier, soil experiences failure (crush) in grains and change in their fabric under high levels of hydrostatic stresses. This phenomenon leads indeed to permanent deformations and consequently plastic behavior in sand specimen at high pressures. Of course, plastic deformations occur in small hydrostatic stresses as well<sup>11</sup>. However, these deformations are so infinitesimal compared to deformations as a result of fabric change. Thus, it can be supposed that under low level of stresses, only elastic deformations occur<sup>6</sup>. Under high pressures, as the loading and fabric change increase in sand specimens, plastic deformations increase accordingly which probably means reduction in the plastic modulus. But on the other hand, by increasing the confining stress and reducing void ratio, this failure (crush) and fabric change ceases gradually and specimen will attain a stability in morphology and arrangement of aggregates; so that by more increase in confining stress, plastic modulus increases gradually. This increasing trend of plastic modulus continues with increase in confining stress until approaching infinity at a bounding mean effective stress  $P_c^{'b}$ . After this level of stress, sand specimen will show behavior like elastic behavior (Lacy and Prevost<sup>4</sup>).

The trend presented above is represented schematically in Figure 1; and three regions can be distinguished from this figure. Initial part of the diagram represents the elastic behavior of the specimen up to the initial state of the cap which occurs at hydrostatic pressure  $p'_0$  (equal to initial distance of the cap from the origin  $k_0$ ). From this

point onward, plastic behavior initiates and increases until the stress approaches a point like  $p_c^{'b}$  (limit point for plastic deformation). Theoretically, after this point, behavior of the sand will return to the elastic state with new fabric characteristics. Moreover, according to experimental observations, transitional part from the initial cap position on the hydrostatic axis  $p'_0$  to  $p_c^{'b}$  can be recognized as a linear part whose slope is  $\lambda_c^b$  and its intercept is  $e_0^b$  (Figures 1 and 2).

By recognition and estimation of the points shown in Figure 1, a relatively exact relationship can be provided for determination of the plastic modulus in hydrostatic loading. Figure 2 illustrates the  $e - \log p'$  curve for Toyoura sand. According to this diagram, initial point for cap performance  $p'_0$  can be observed.

However, the position of  $p_c^{'b}$  is at a very high level of stress; and it's practically difficult to approach this position of stress due to experimental limitations. In addition, since

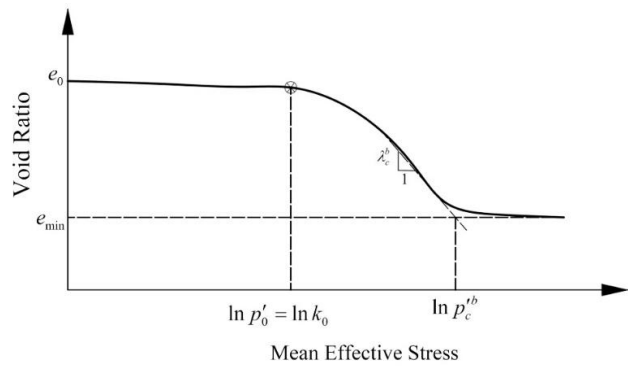


**Figure 1.** Schematic representation of diagram  $e - \log p'$  in a hypothetical hydrostatic loading (loading from low to very high pressures).

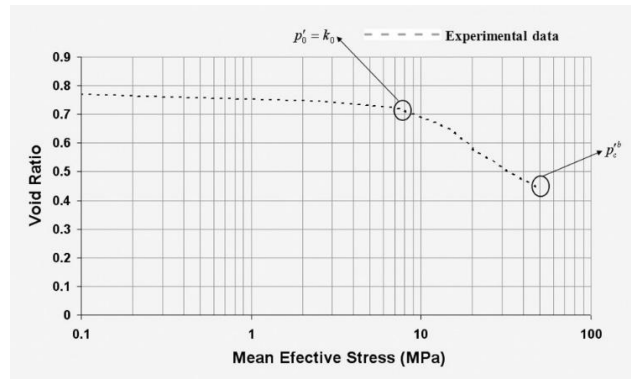


**Figure 2.** Experimental data for Toyoura sand on the plane of  $e - \log p'$ .

in practice, we rarely face these very high levels of stresses, available experimental data seldom has approached these values. Therefore, it is assumed that the value of the cap plastic modulus will start from a value and approach infinity at a bounding mean effective stress  $p_c^{b}$ . Thus, following relationship is proposed for the cap plastic modulus:

$$H_2^p = \bar{H}_2^{-1} \left( \frac{p'}{\langle p_c^{b} - p' \rangle} \right)^{0.5} \quad (11)$$

where,  $H_2^p$  is the plastic modulus in hydrostatic loading,  $\bar{H}_2^{-1}$  is a constant coefficient which is calibrated based on experimental data corresponding to the soil and  $p_0'$  is the starting point of the plastic behavior.  $p_c^{b}$  is the hypothetical position of the bounding surface of the cap which is estimated by means of the experimental data of the soil. Value of  $p_c^{b}$  is estimated using the following relationship

$$p_c^{b} = \text{Exp} \left( \frac{e_0^b - e_{\min}}{\lambda_c^b} \right) \quad (12)$$

where,  $\lambda_c^b$  is slope and  $e_0^b$  is the intercept of the soil fabric change line and  $e_{\min}$  is the minimum intended void ratio for a soil.

## 2.2 Yield and Hardening Functions

Yield function of the first mechanism, is a cone in the principle stresses space so that the vertex of the cone is on coordinate axes. Moreover, in the first mechanism, kinematic hardening law is used. Equations corresponding to this mechanism are presented in<sup>3-6,12</sup>.

However, in the definition of the second yield function, cap plasticity function is assumed to be volumetric. The cap makes a yield surface normal to the hydrostatic axis in stress space; so this yield surface closes the conical yield and bounding surfaces as a cap (Figures 3 and 4). Cap function is expressed simply in stress space (and  $q - p'$  plane) as follows:

$$f_2 = p' - k \quad (13)$$

where,  $p'$  is the current mean effective stress and  $k$  denotes the position of the cap yield surface on hydrostatic axis. Therefore, vector normal to the cap is in the form of a Kronecker vector:

$$L_{ij}^2 = \delta_{ij} \quad (14)$$

It is not far from reality that the hardening of the cap yield surface is considered only as the isotope hardening

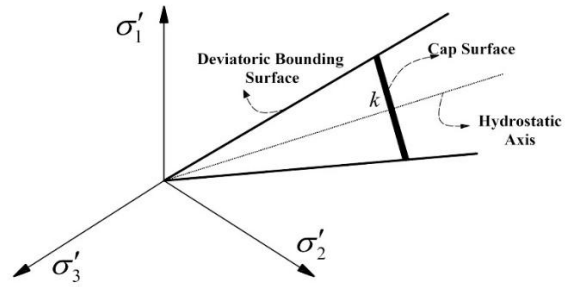


Figure 3. Schematic bounding and cap surfaces in the principle stresses space.

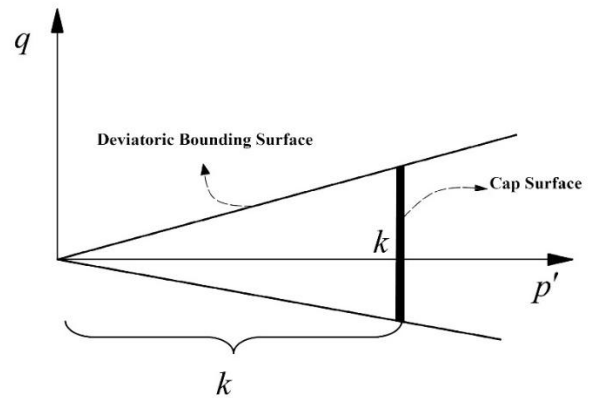


Figure 4. General representation of the yield surface of the cap in  $q - p'$  stress space.

since plastic deformations as a result of confining pressure at high stress are attributed mainly to the failure (crush) of grains and change in the fabric of specimens<sup>6</sup>. If we neglect plastic deformations in case of low hydrostatic pressures and in such conditions, deformations are assumed to be merely elastic, after the first hydrostatic loading stage at high stress levels and approaching the yield surface of the cap, sand particles will be approximately crushed and the sand fabric of will change. By unloading, changes made in the fabric will remain and soil will show a behavior similar to the elastic behavior during unloading. In reloading, since specimen particles failed at high stress levels, we observe negligible plastic deformation as a result of failure (crush) in specimen particles. Experimental results confirm this finding<sup>13</sup>. Of course, it must be noted that the most of constitutive models which have cap, follows hardening law as well<sup>14,15</sup>. In this way, changes in the position of the cap surface will be computed as follows:

$$dk = \frac{H_2^p}{3} < \lambda_2 > \quad (15)$$

It means that when the stress position is on the cap, value of the yield surface changes in such a way that surface of the cap will always match the maximum mean effective stress experienced by the soil. In other words,  $k$  changes so that it doesn't exceed the cap surface. For determining the surface equation of the cap, it is necessary that the  $k$  is evaluated. According to the experimental data, it is evident that initial position of the cap for the volumetric plastic behavior is related to the void ratio of the sand specimens and is along with bounding line of the fabric. Therefore, initial location of the cap in hydrostatic loading is defined as follows:

$$k_0 = a_1 \text{Exp}\left(\frac{e_0^k - e}{\lambda_c^b}\right) \quad (16)$$

where, parameters  $a_1$  and  $e_0^k$  are constants of the model whose best value can be obtained through calibration of the model by experimental data and  $e$  is the void ratio of the soil which can be considered as the initial void ratio.

### 3. Evaluation of the Performance of the Cap in Constitutive Model (By Experimental Data)

Parameters required for the model corresponding to the cap which are added to the main constitutive models are: slope and intercept of the bounding line of the soil fabric change (i.e.  $e_0^b$  and  $\lambda_c^b$ ), minimum void ratio of the intended soil  $e_{\min}$ ,  $e_0^k$  as a parameter for determining the initial position of the cap surface,  $\overline{H}_2^{-1}$  as the constant of the plastic modulus of the cap. To assess the algorithm and mechanism presented for cap, it is important to calibrate the required parameters for a soil according to experimental data. For this purpose, experimental data presented by<sup>7</sup> and Salazar<sup>8</sup> for Toyoura and Nevada sands respectively, are used.

The tests carried out on Toyoura sand include three series of experimental hydrostatic data at high pressures which are measured in three void ratios: 0.83, 0.77 and 0.59. Further, the data corresponding to Nevada sand specimens with void ratios of 0.72 and 0.49 have been presented. The required model parameters have been calibrated for this sands and summarized in Table 1.

Now, according to values presented in Table 1, the simulations of the main constitutive model without cap as well as the modified model with cap compared to experimental data are illustrated in Figures 5, 6, 7 and 8. Figures 5

**Table 1.** Parameters of the calibration of the model for experimental data of Toyoura sand

Parameters	sand Toyoura	sand Nevada
K (kPa)	50000	60000
G (kPa)	50000	60000
$\lambda_c^b$	0.154	0.2
$e_0^b$	1.164	1.33
$e_0^k$	1.118	1.2
$\overline{H}_2^{-1}$	50000	100000

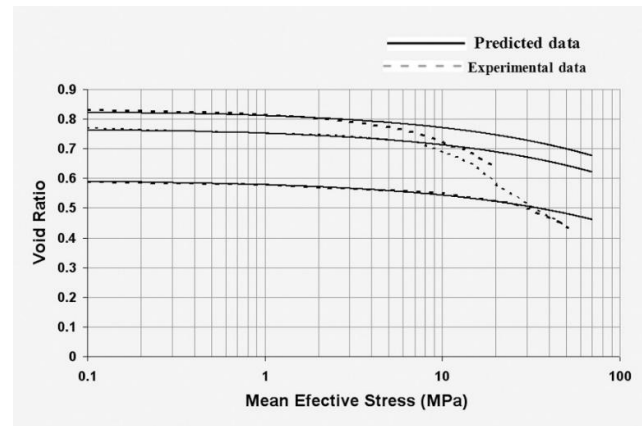


**Figure 5.** Results of the prediction of constitutive model without cap compared to results of experiment at high pressures on Toyoura sand.

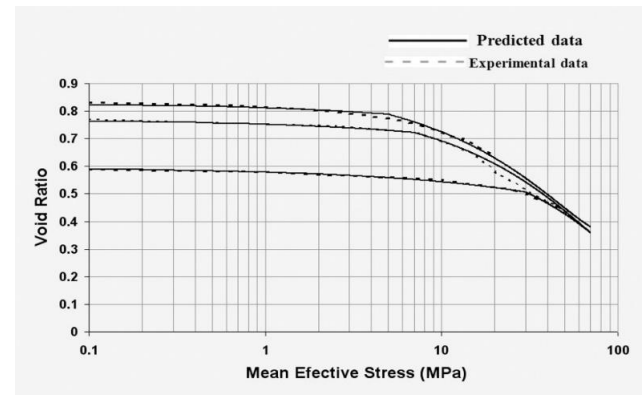


**Figure 6.** Results of the prediction of corrected constitutive model with cap compared to results of experiment at high pressures on Toyoura sand.

and 7 represent the predictions of the main constitutive model by Manzari and Dafalias<sup>4</sup> before adding the cap for Nevada and Toyoura sands. It is observed that constitutive model without cap cannot show the behavior of soil at high pressures. In Figures 6 and 8 which correspond

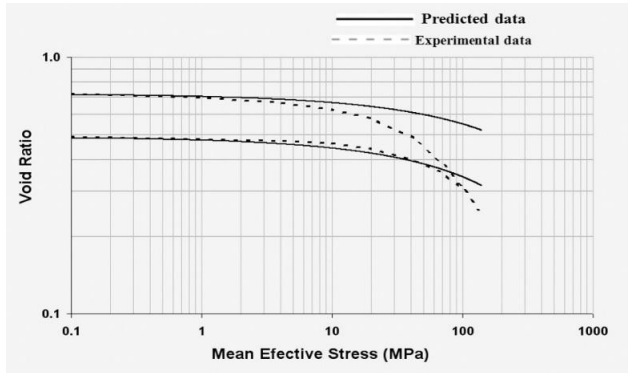


**Figure 7.** Results of the prediction of constitutive model without cap compared to results of experiment at high pressures on Nevada sand.

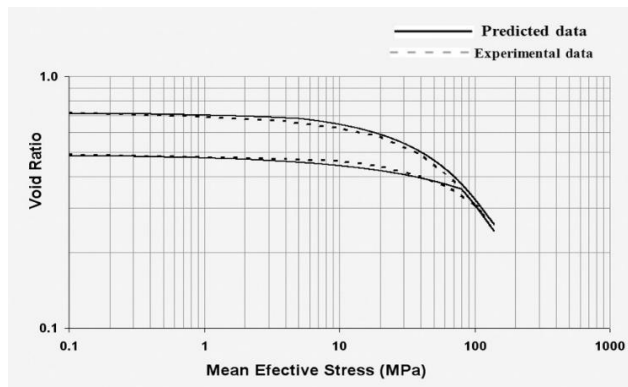


**Figure 8.** Results of the prediction of corrected constitutive model with cap compared to results of experiment at high pressures on Nevada sand

to the prediction of the modified constitutive model with cap, it can be obviously seen that the modified model can show the behavior of the soil at very high pressures. In other words, the simulations of the modified constitutive model have satisfactory agreement with experimental data.

## 4. Conclusion

The constitutive models are considered as one of the most suitable advanced models for prediction of sand behavior. These models are presented in the framework of the bounding surface plasticity. One of the weaknesses of the constitutive models is that they don't have cap and therefore, they fail to simulate appropriately the behavior of sands at high pressures in which failure (crush) in

particles occur. We added an appropriate cap for high level of pressure into the algorithm of the main constitutive model; so that the model can simulate the plastic deformation behavior resulted from hydrostatic especially at very high pressures in an appropriate manner. High pressures occur mainly in projects such as construction of high dams; and if the constitutive model of the soil at such pressures cannot be modeled well, considerable errors will occur in computations.

Then, formulation of a cap has been added to an advanced constitutive model. The modified model has been calibrated based on experimental data corresponding to two various sands; Toyoura and Nevada. In this way, the predictions of the constitutive models before and after modification were presented according to experimental data. It has been observed the model modified by cap are able to predict the behavior of the sand at high pressures in which sand particles fail (crush). Whereas, the primary model (without a cap for high pressures) is not capable to show sand behavior at high level of stresses.

## 5. References

1. Monfared V, Fazaeli D, Daneshmand S, Shafaghatian N. Simulation of Elasto-plastic Deformations in Composites by Flow Rules. *Indian Journal of Science and Technology*. 2014 Feb; 7(2):180–84.
2. Yamamuro JA, Bopp PA, Lade PV. One-Dimensional Compression of Sand at High Pressures. *Journal of Geotechnical Engineering*. 1996; 122:147–53.
3. Manzari MT. Davis: University of California: Finite Deformation Analysis and Constitutive Modeling of Non-Cohesive Soils for Liquefaction Problems. Doctoral thesis. 1994.
4. Manzari MT, Dafalias YF. A critical state two-surface plasticity model for sands. *Geotechnique*. 1997; 47:255–72.
5. Tamagnini R. An extended cam-clay model for unsaturated soils with hydraulic hysteresis. *Geotechnique*. 2004; 54:223–28.
6. Lacy SJ, Prevost JH. Constitutive Model for Geomaterials. *Proceedings 2nd International Conference on Constitutive Laws for Engineering Materials*. Elsevier. 1987; 1:149–60.
7. Miura N, Murata H, Yasufuku N. Stress-Strain Characteristics of Sand in a Particle-Crushing Region. *Soils and Foundations*. 1984; 24:77–89.
8. Salazar SE. The University of Arkansas: College of Engineering: One-Dimensional Compressibility of Intermediate Non-Plastic Soil Mixtures. Thesis in Department of Civil Engineering. 2013.

9. Heidarzadeh H. Tehran: University of Tehran: Comparison of Different State Parameters Effect on the Improvement of an Elastoplastic Model Predictions. M.Sc Thesis in geotechnical engineering. 2010.
10. Heidarzadeh H, Latifi M. Evaluation of different state parameters' Effect on Modification of a Bounding Surface Elasto-plastic Model. Sharif Journal (Civil Engineering). 2012; 28:57-64.
11. Ko HY, Scott, RF. Deformation of Sand in Hydrostatic Compression. Journal of the Soil Mechanics and Foundations Division. 1967; 93:137-57.
12. ParvezIqbal A, Rahman M, Norhisam Misron M. Design and Optimization of the Housing of Spray Unit of a Linear Motor Operated Spray Gun, Indian journal of science and technology, 2013 Aug; 6(8):88-94.
13. Lade PV, Yamamuro JA. Drained Sand Behavior in Axisymmetric Test at High Pressures. Journal of Geotechnical Engineering. 1996; 122:120-29.
14. Dhas L, Raguraman D, Muruganandam D, Senthilkumar B. Indian Journal of Science and Technology. 2015 Nov; 8(31):68-74.
15. Tabatabaei M, Solaimani K, Habibnejad Roshan MH, Kaviani A. Daily Suspended Sediment Load Estimation by Meta-heuristic Optimization Approaches and Fuzzy-C-means Clustering Method. Indian Journal of Science and Technology. 2014; 7:1488-97.